

https://doi.org/10.1070/QEL17347

Homogeneous broadening in the spectrum of a broadband erbium-doped fibre light source

S.K. Morshnev, N.I. Starostin, Ya.V. Przhiyalkovsky, A.I. Sazonov

Abstract. **Interference of wave trains separated out in an inhomogeneous emission spectrum of a superluminescent erbium-doped fibre source has been studied by scanning the wavelength of a spectrum analyser. The results demonstrate that, as the spectral resolution of the spectrum analyser decreases to a level corresponding to a sharp drop in interference fringe visibility relative to its original level, near 100 %, fringe visibility becomes dependent on the wavelength in the inhomogeneous spectrum of the source. The reason for this is that, at some characteristic resolution $\delta\lambda$ ($\delta\lambda > 0.5$ nm in our case), the coherence time of wave trains is not limited by the spectral resolution of the spectrum analyser and is related to the inhomogeneous spectrum of the source, whose limiting width can be thought of as the homogeneous linewidth in the spectrum of the source. This feature can be used for evaluating homogeneous line broadening.**

Keywords: *homogeneous broadening, interference visibility, coherence time.*

1. Introduction

Fibre-optic current and angular rate sensors based on reciprocal interferometers utilise broadband optical sources, including erbium-doped fibre sources [1, 2]. If the optical power incident on a photodetector exceeds 10 μW, the main noise component of such sources is excess noise, which in this case determines the sensitivity limit of the interferometric sensor [2]. Excess noise is a linear function of optical power, which prevents the signal-to-noise ratio from being raised by increasing the optical power incident on the photodetector. This type of noise is known to be related to heterodyne beating between two neighbouring spectral components of a light source [3, 4]. Excess noise results from such a beat with a random phase. The broader the spectrum of a source, the higher is the probability to find a pair with the same frequency and the opposite phase and the lower is the excess noise. In the case of an inhomogeneously broadened spectrum of an erbium-doped light source, it is reasonable to assume that heterodyne beating involves homogeneously broadened lines. The excess noise level of a broadband source can then depend on not only its emission bandwidth but also the structure of its spectrum [3, 4], which makes it important to study the structure of an inhomogeneous spectrum of a light source.

In classical spectroscopy, the ability to separate the contributions of homogeneous and inhomogeneous broadening in spectra is a serious problem even in the case of crystalline media, and the picture of broadening is significantly more complex for disordered solids (amorphous structures, polymers, and glass, as in our case), so that it is not always possible to separate the contributions of homogeneous and inhomogeneous broadening. In spectroscopy, they are often separated by rather complex methods, using low (cryogenic) temperatures, selective laser excitation, spectral hole burning [5–7], and selective spectroscopy of single molecules [8, 9]. For this reason, the ability to separately assess homogeneous broadening in spectra of various sources continues to be a topical issue.

The inhomogeneous spectral bandwidth of superluminescent erbium-doped sources is ~20 nm. It is determined by the facts [10–12] that (1) the ground state of trivalent erbium ions is the $^4I_{15/2}$ term, with a rich multiplet structure due to the Stark effect in the electric field of the nearest neighbour environment of the Er^{3+} ion [11]; (2) the excited state ($^4I_{13/2}$ term) responsible for the luminescence is also highly split (for the same reason); and (3) glassy short-range 'crystal lattices' of silica fibre differ in 'crystal field'. To the best of our knowledge, there are still no reports on the determination of the width of homogeneously broadened components in the spectrum of broadband superluminescent erbium-doped sources.

We propose a comparatively simple method for evaluating the homogeneous broadening in the envelope of an inhomogeneously broadened spectrum of a source. The method consists in using filters differing in spectral width in order to produce wave trains with different coherence times, comparable to the artificial time delay in a fibre-optic line, and use their interference fringe visibility for assessing the degree of monochromaticity of the trains. We used filters with a variable spectral bandwidth. The idea of filtering light for improving fringe visibility has long been used (e.g. in the Rayleigh and Jamin interferometers, which use light from incandescent lamps [13]).

2. Experimental

2.1. Concept of the experiment

It is known [14, 15] that a receiver with a controlled spectral resolution $\delta\nu$ can act as a tunable spectral filter of bandwidth $\delta\nu$. Varying the resolution, we can separate out wave trains

S.K. Morshnev, N.I. Starostin, Ya.V. Przhiyalkovsky, A.I. Sazonov
Kotelnikov Institute of Radio Engineering and Electronics (Fryazino Branch), Russian Academy of Sciences, pl. Vvedenskogo 1, 141190 Fryazino, Moscow region, Russia;
e-mail: morshnev@profotech.com, nis229@ire216.msk.su

Received 10 April 2029; revision received 19 June 2020
Kvantovaya Elektronika **50** (10) 904–909 (2020)
Translated by O.M. Tsarev

with different coherence times, $\tau = 1/\delta\nu$, in the spectrum, or (in terms of wavelengths λ)

$$\tau = \frac{\lambda^2}{c\delta\lambda}, \tag{1}$$

where c is the speed of light in vacuum and $\delta\lambda$ is the transmission bandwidth of the filter. Increasing $\delta\lambda$ leads to a decrease in the coherence time $\tau\lambda$ of wave trains that are received by the receiver. One possible receiver is a Yokogawa AQ6370C spectrum analyser with a set of discrete spectral resolutions $\delta\lambda$ from 0.02 to 2 nm, which allows the coherence time of wave trains to be varied over two orders of magnitude.

Let t_x (or t_y) be the time needed for a wave train polarised along the x (or y) axis to pass through a delay line. Introducing a time delay $(t_y - t_x)$ between two orthogonally polarised wave trains and causing them to interfere, we can monitor the degree of overlap of the wave trains from fringe visibility V. In the simplest case of a constant amplitude throughout a wave train, we have

$$V \approx 1 - \frac{t_y - t_x}{\tau}. \tag{2}$$

Interference fringes can then be observed using the same Yokogawa AQ6370C spectrum analyser, with a wavelength sweep. The visibility function $V(\lambda)$ can be determined for a particular wavelength λ_{av} between the wavelengths of a maximum and a minimum in the interference pattern (IP) within the spectrum of the source. At a small transmission bandwidth of the filter ($\delta\lambda$), fringe visibility is constant throughout the spectrum of the source and is only determined by the overlap between wave trains [see (2)]. If the coherence time τ is determined by the transmission spectrum of the filter according to relation (1), an increase in $\delta\lambda$ leads to a reduction in the coherence time, the overlap between wave trains, and hence visibility V, which is constant throughout the spectrum of the source.

In this situation, the homogeneous structure of the spectrum of the source does not show up, and all is determined by the spectral bandwidth of the filter of the receiver.

The spectral width $\delta\lambda_{hom}$ of homogeneously broadened lines of the source also can limit the coherence time of wave trains received, if the spectral bandwidth of the filter exceeds the homogeneously broadened linewidth. In this case, the coherence time of a wave train is determined by the homogeneous linewidth in a given part of the spectrum. Clearly, the width of different homogeneously broadened lines can vary from one part of the spectrum to another, causing visibility $V(\lambda)$ to vary with wavelength within the spectrum of the source. Finally, if the transmission band of the filter contains a few homogeneous lines, the inhomogeneous properties of the spectrum of the source will show up in this spectrum.

If the spectrum of the source controls the visibility function $V(\lambda)$ over the entire spectrum and the transmission bandwidth $\delta\lambda$ of the filter of the receiver is just above a certain value, $\delta\lambda_{hom}$, it is reasonable to conclude that $\delta\lambda_{hom}$ is the homogeneous linewidth of the source.

In addition, the previously observed sharp drop in visibility for $\delta\lambda > \delta\lambda_{hom}$ [16] becomes explainable. In this case, the transmission band of the receiver contains more than one homogeneously broadened line with a different resonance frequency. As a result of interference, we obtain two or more IPs differing in frequency. This leads to a reduction in the visibility of the total IP. Thus, we obtain an additional mechanism, found previously [16], of the drop in visibility. It is reasonable to consider the $\delta\lambda$ at which this dependence appears as the homogeneously broadened linewidth $\delta\lambda_{hom}$ of the source and, at the same time, as the limiting width of its inhomogeneous spectrum.

2.2. Experimental implementation

Figure 1 shows a schematic of the experimental setup. Light at the output of the superluminescent erbium-doped fibre source (*1*) has an inhomogeneous spectrum ~20 nm in width (Fig. 2). After passing through a fibre polariser (*2*), the light is linearly polarised. The 45° splice at point *3* connects the output of the polariser (*2*) and the input of a hi-bi fibre delay line (*4*) $z = 3.5$ m long. As a result, the plane of the polariser (*2*) is oriented at 45° with respect to the built-in birefringence (BR) axes of the hi-bi fibre (beat length $L_b \approx 3$ mm). This orientation ensures that wave trains polarised along the x and y axes of the BR fibre in the delay line (*4*) have equal amplitudes. Owing to the built-in BR, the propagation velocity of wave trains polarised along the x axis is $v_x = c/n_x$, and that of wave trains polarised along the y axis is $v_y = c/n_y$, where n_x and n_y are the refractive indices for waves linearly polarised along the x and y axes. Light whose spectrum is limited by a filter with a bandwidth $\delta\nu$ can be represented as a set of wave trains with a coherence time $\tau \approx 1/\delta\nu$ [15]. The wave trains polarised along the x axis will be delayed in the delay line (*4*) for time $t_x = z/v_x = zn_x/c$, and those polarised along the y axis will be delayed for time $t_y = z/v_y = zn_y/c$. As a result, one type of wave train will be delayed relative to the other for time

$$t_y - t_x = (n_y - n_x)z/c, \tag{3}$$

with a phase shift

$$\Delta\varphi = k_0(n_y - n_x)z = 2\pi\nu(n_y - n_x)z/c, \tag{4}$$

where $k_0 = 2\pi\nu/c$ is the wavenumber in vacuum and ν is the frequency of the light wave.

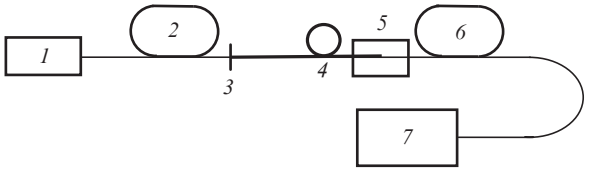

Figure 1. Schematic of the experimental setup: (*1*) superluminescent erbium-doped fibre source; (*2*) fibre polariser; (*3*) 45° splice; (*4*) PM fibre delay line; (*5*) Ericsson FSU 995 PM splicer; (*6*) fibre polariser (analyser); (*7*) Yokogawa AQ6370C spectrum analyser.

It is known [13] that wave trains with orthogonal polarisations cannot interfere. To observe interference, one should ensure that their polarisation vectors have, as far as possible, equal projections onto the transmission plane of the fibre polariser (analyser) (*6*), i.e. that the transmission plane of the polariser is oriented at 45° with respect to the built-in BR axes of the hi-bi fibre. To improve angular orientation accuracy, rotation of the hi-bi fibre (*4*) relative to the fibre of the analyser (*6*) is ensured by manual angle alignment of the Ericsson

FSU 995 PM splicer (*5*). At the output of the analyser (*6*), we have

$$E = E_x(t)\cos(\omega t - k_0 n_x z) + E_y(t)\cos(\omega t - k_0 n_y z), \qquad (5)$$

where $E_x(t)$ and $E_y(t)$ are the slowly varying (compared to frequency ω) amplitudes of wave trains. The detector of the spectrum analyser (Yokogawa AQ6370C) (*7*), with a response time T_D, detects intensity $I(\lambda)$:

$$I(\lambda) = \frac{1}{T_D}\int_0^{T_D} E^2 \mathrm{d}t = \frac{1}{T_D}\int_0^{\tau} \frac{E_x^2(t) + E_y^2(t)}{2}\mathrm{d}t$$

$$+ \frac{1}{T_D}\cos[k_0(n_y - n_x)z]\int_0^{\tau-(t_y-t_x)} E_x(t)E_y(t)\mathrm{d}t. \qquad (6)$$

It should be emphasised that, with allowance for the coherence time τ of the wave trains and their time difference, the upper integration limit in the first term of (6) is τ, and that in the second term is the wave train overlap time, $\tau - (t_y - t_x)$. Relation (6) can be written in the form

$$I = I_0\{1 + V\cos[k_0(n_y - n_x)z]\}, \qquad (7)$$

where

$$I_0 = \int_0^{\tau} \frac{E_x^2(t) + E_y^2(t)}{2T_D}\mathrm{d}t, \qquad (8)$$

$$V = \frac{\int_0^{\tau-(t_y-t_x)} E_x(t)E_y(t)\mathrm{d}t}{\frac{1}{2}\int_0^{\tau} E_x^2(t) + E_y^2(t)\mathrm{d}t}. \qquad (9)$$

As seen from (9), fringe visibility depends on the degree of overlap of wave trains. If the time delay between wave trains $(t_y - t_x)$ exceeds their coherence time τ, they do not overlap at the detector input and fringe visibility is zero. At a high resolution [$\tau \gg (t_y - t_x)$], wave trains with initially orthogonal polarisations almost completely overlap at the detector input, ensuring high fringe visibility.

Interference on the display of the spectrum analyser (*7*) is observed with a wavelength sweep. The argument of the cosine in (7) is inversely proportional to λ:

$$k_0(n_y - n_x)z = 2\pi\lambda_{av}\frac{z}{L_b}\frac{1}{\lambda}, \qquad (10)$$

where $(n_y - n_x) = \lambda_{av}/L_b$; λ_{av} is the average wavelength in experimental determination of the beat length L_b [17]; and λ is the wavelength at which intensity $I(\lambda)$ is determined.

2.3. Experimental data processing

Figure 2 shows the output spectrum $F(\lambda)$ of the superluminescent Er^{3+}-doped fibre source used in our experiments. $F(\lambda)$ varies continuously, which prevents us from determining fringe visibility using the well-known formula $V = (I_{max} - I_{min})/(I_{max} + I_{min})$. This is confirmed by the typical IP on the display of the spectrum analyser (*7*) at a resolution $\delta\lambda$ = 0.5 nm (Fig. 3).

We use a correction factor A for the $F(\lambda)$ spectrum because the output intensity depends on the spectral bandwidth of the filter, fusion splice quality, and the 45° orientation of the birefringence axes of the fibre (*4*) relative to the transmission plane of the polariser (*6*) (Fig. 1). Taking into account the above and using relations (7) and (10), we obtain for the IP intensity

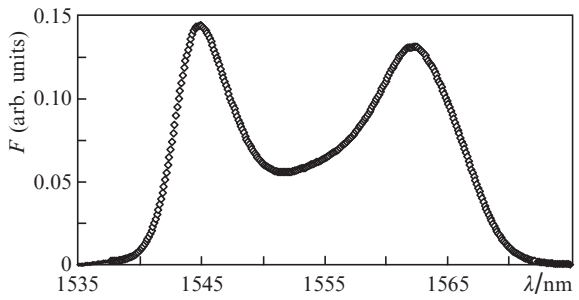

Figure 2. Output spectrum $F(\lambda)$ of the superluminescent erbium-doped fibre source.

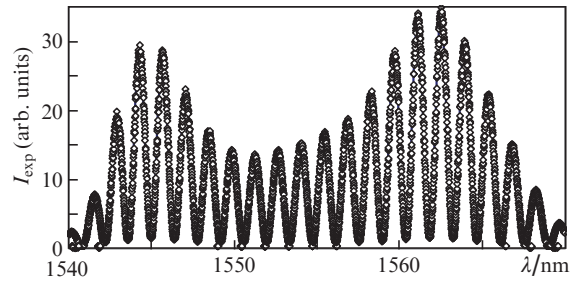

Figure 3. Typical IP on the display of the spectrum analyser (*7*) in an experiment at a resolution $\delta\lambda$ = 0.5 nm.

$$I_{exp}(\lambda) = AF(\lambda)\left[1 + V\cos\left(2\pi\lambda_{av}\frac{z}{L_b}\frac{1}{\lambda} + \varphi_0\right)\right]$$

$$= I_{theor}(A, V, L_b, \varphi_0, \lambda). \qquad (11)$$

$I_{exp}(\lambda)$ is measured experimentally (Fig. 3), and the right-hand part of (11) is adjusted so as to minimise the rms deviation from the left-hand part using A, V, L_b, and φ_0 as fitting parameters. The large number of such parameters should not bother us because they are in significant measure independent of each other. To exclude the dependence on the parameters L_b and φ_0, we turn to the maximum and minimum values of $I(\lambda)$:

$$I_{max} = AF(\lambda)(1 + V),$$

$$I_{min} = AF(\lambda)(1 - V). \qquad (12)$$

These values are reached when the cosine in (11) is +1 and –1, respectively. Consider how the corrections ΔA and ΔV influence the parameters of (12). We denote the uncorrected parameters in (12) as $I_{max\,0}$ and $I_{min\,0}$. The corrected parameters are then given by

$$I_{max} = I_{max\,0}\left(1 + \frac{\Delta A}{A} + \frac{\Delta V}{1 + V}\right), \qquad (13)$$

$$I_{\min} = I_{\min 0}\left(1 + \frac{\Delta A}{A} - \frac{\Delta V}{1 - V}\right). \tag{14}$$

It is seen from (13) and (14) that the corrections to $I_{\max}$ and $I_{\min}$ are proportional to $\Delta A/A$ for both quantities, but the correction to $I_{\max}$ is proportional to $I_{\max 0}\Delta A/A$, whereas that to $I_{\min}$ is proportional to $I_{\min 0}\Delta A/A$, with $I_{\max 0} \gg I_{\min 0}$. Thus, ΔA influences mainly $I_{\max}$. A change in visibility, ΔV, in turn has a stronger effect on $I_{\min}$ [proportional to $\Delta V/(1 - V)$] than on $I_{\max}$ [proportional to $\Delta V/(1 + V)$]. At $V \approx 1$, the effect on $I_{\min}$ can be very strong. As an illustration, consider Fig. 4. It shows experimentally obtained IPs with a highly expanded wavelength axis in the region of $I_{\min}$ at $\delta\lambda = 0.1$ nm. The solid lines represent theoretical fits to (11) at $V = 0.999$ and 0.992. It is seen even without calculating rms deviations that the experimental data are better described by the theory at $V = 0.992$. Thus, in the region of $V \approx 1$, V can be selected with high accuracy.

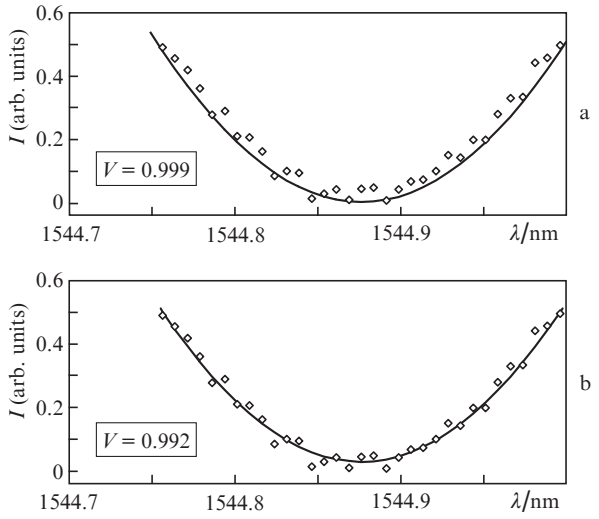

Figure 4. Portion of the region of a minimum in an IP at $\delta\lambda = 0.1$ nm with a highly expanded wavelength axis. The open squares are the experimental data and the solid lines represent the right-hand side of (12) with the best fit parameters A, L_b, φ_0, and V = (a) 0.999 and (b) 0.992.

We now turn to phase parameters. If the minima and maxima in an IP are shifted along the wavelength axis, one should change the parameter φ_0. The entire IP will then shift in the spectrum as a whole. At the same time, if the shifts of the maxima (minima) along the wavelength axis do not coincide even in neighbouring regions of the spectrum, one should change the beat length L_b and again select the parameter φ_0 so as to cause neighbouring minima and maxima to coincide.

Each IP, e.g. that shown in Fig. 3, contains 10 000 experimental data points with a noticeable noise component (5% to 10%) and well-defined maxima and minima. To improve visibility $V(\lambda)$ determination accuracy, we used the following technique: As a basis, we took relation (11), where the $I_{\exp}(\lambda_i)$ data points were taken to be the left-hand part, whereas in the right-hand part, $I_{\text{theor}}(A, V, L_b, \varphi_0, \lambda_i)$, we adjusted the parameters A, V, L_b, and φ_0 so as to minimise the rms deviation γ of the $I_{\exp}(\lambda_i)$ data points from the theoretical function $I_{\text{theor}}(A, V, L_b, \varphi_0, \lambda_i)$ at the same wavelength:

$$\gamma = \sqrt{\frac{1}{N}\sum_{i=1}^{N}[I_{\exp}(\lambda_i) - I_{\text{theor}}(\lambda_i)]^2}\,. \tag{15}$$

The summation was carried out in the vicinity of point λ_{av}, which was chosen among the points of the maxima or minima. The vicinity of the point chosen was taken to consist of two IP periods in the short-wavelength part and two IP periods in the long-wavelength part (a total of about 500 data points). They were used to minimise γ in the following sequence: (1) minimisation with respect to A and V; (2) shift along φ_0, (3) verification of the periods and minimisation with respect to L_b, (4) another shift along φ_0 in the case of a change in L_b, and (5) another minimisation with respect to A and V. The number of such cycles was equal to the number of periods in the spectrum of the IP, and the period $\Delta\lambda$ was evaluated from the beat length L_b [17]:

$$\Delta\lambda = \frac{L_b}{z}\lambda_{av}. \tag{16}$$

The experimental data processing results are presented in Fig. 5. Figure 5a shows spectral dependences of fringe visibility at different resolutions of the spectrum analyser: $\delta\lambda$ = 0.05, 0.1, 0.2, and 0.5 nm. For comparison, the solid line shows the output spectrum of the superluminescent source. It is seen that, at filter bandwidths of 0.05, 0.1, and 0.2 nm, fringe visibility is wavelength-independent and its decrease is due to the decrease in the coherence time τ of wave trains, whose spectrum is determined by the filter (at a constant delay time). All is consistent with Eqns (1)–(3) and previous results [16]. Radically different behaviour is exhibited by fringe visibility at $\delta\lambda = 0.5$ nm (Fig. 5a). In addition to a sharp decrease, visibility depends on wavelength, and the deviation of $V(\lambda)$ from the average over the spectrum of the source reaches ~3%. Here, the properties of the light source begin to show up, including the homogeneous broadening of its spectrum, which in general depends on wavelength. Further increasing the spectral bandwidth of the filter (reducing the resolution of the spectrum analyser) leads to a further decrease in visibility $V(\lambda)$ and an increase in its deviation from the average over the spectrum of the source. At $\delta\lambda = 1.0$ nm, the deviation reaches almost 11% (Fig. 5b). In addition, there is a large scatter in $V(\lambda)$, exceeding its average at $\delta\lambda = 2.0$ nm (Fig. 5c).

All the above supports the assumption that a different mechanism, related to interference, comes into play: superposition of two or more IPs of homogeneous source emission lines differing in wavelength. This mechanism shows up when the spectrum of a wave train separated out by the filter of the receiver is broader than the spectrum of a homogeneous line of the source. The larger the number of homogeneous lines involved in interference, the lower the fringe visibility. This is a manifestation of the inhomogeneity of the spectrum in the $\delta\lambda$ range.

The increase in fringe visibility at the short- and long-wavelength edges of the spectrum of the source can also be accounted for by the fact (Fig. 5c) that, at the edges, the limitation imposed on the width of the spectrum by the resolution of the spectrum analyser, $\delta\lambda$, is further enhanced by the edges of the spectrum of the source. The spectral width of the separated wave train becomes smaller than the resolution, $\delta\lambda_{\exp} < \delta\lambda$, and this improves visibility $V(\lambda)$ (see above) at the edges of the spectrum of the source.

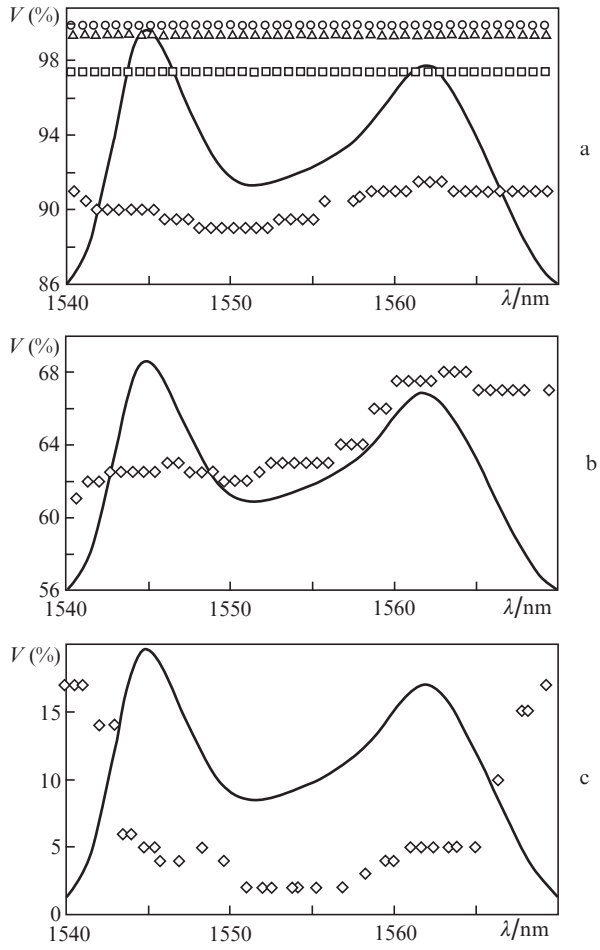

Figure 5. Fringe visibility $V(\lambda)$ as a function of the position in the spectrum of the source at $\delta\lambda$ = (a) 0.05 (○), 0.1 (△), 0.2 (□), 0.5 (◇), (b) 1.0, and (c) 2.0 nm. For comparison, the solid line shows the emission spectrum of the source.

3. Discussion

We proposed a comparatively simple method for assessing an important parameter of the structure of the spectrum of a broadband light source: its homogeneous bandwidth $\delta\lambda_{hom}$. The superluminescent erbium-doped fibre source used by us has $\delta\lambda_{hom} = 0.5$ nm. According to (1), the corresponding coherence time of wave trains from the source is $\tau = 1.6 \times 10^{-11}$ s, and the wave train length in vacuum is $L_z = 4.8$ mm (which far exceeds λ). The values of τ and L_z can be estimated using inequalities. Indeed, at $\delta\lambda = 0.2$ nm there are no signs of inhomogeneity and no effect of the spectrum of the source on visibility ($V = 0.974$). It is reasonable to assume that the resolution coincides with the homogeneous linewidth: $\delta\lambda = \delta\lambda_{hom}$. Then, we have $0.2 < \delta\lambda_{hom} < 0.5$ nm, $1.6 \times 10^{-11} < \tau < 4.0 \times 10^{-11}$ s, and $4.8 < L_z < 12$ mm.

Besides, an increase in the spectral width of observed wave trains was accompanied by a sharp drop in fringe visibility. We attributed it to the overlap of IPs due to different homogeneous lines offset relative to each other in the spectrum (manifestation of the inhomogeneity of the source).

The present results allow us to make a number of clarifications regarding the excess noise of the source under study. As pointed out in Section 1, excess noise results from heterodyne beating between spectral components of light from a broadband source [3, 4]. The excess noise level depends on the inhomogeneous spectral width of the light source. This can be accounted for by the different numbers of spectral components involved in beating. In doing so, it is assumed that the spectral components are monochromatic and that only for them can the concept of phase be introduced. A monochromatic component has a narrow spectrum determined by its coherence time. At the same time, the phase of the component is thought to be a random value, which is in general understandable: in different parts of the spectrum, monochromatic lines begin generation absolutely at random. As a result, the average excess noise due to the 'heterodyne' mechanism proves to be proportional to the spectral width of the source. Thermal sources, e.g. those with a very broad inhomogeneous spectrum, have very low excess noise [4].

At the same time, the notion of an inhomogeneous spectrum as a set of monochromatic components is an idealisation. As found out by us, the homogeneous spectral width of the source is sufficiently large, which leads to two consequences: (1) there is a finite number of homogeneous lines in the spectrum of the source and (2) the excess noise level is inversely proportional to the number of homogeneous lines in the emission spectrum of the source and can vary at a given inhomogeneous emission linewidth.

Unfortunately, we had to reject the quantitative use of $V(\delta\lambda)$ data relying e.g. on previous results [18], even though such an attempt was made in Ref. [16], which, in particular, presented $V(\delta\lambda)$ data. This is due to the lack of information about the shape of a homogeneous line cut by the spectrum analyser, as well as to the complex nature of the inhomogeneous spectrum of the erbium-doped source (due to the large number of luminescence transitions).

4. Conclusions

We have proposed a simple method for assessing the spectral width of a homogeneous line in the inhomogeneous spectrum of a broadband superluminescent erbium-doped fibre source. It uses the discrete controlled resolution $\delta\lambda$ of a Yokogawa AQ6370C spectrum analyser as a filter for separating out wave trains differing in coherence time. Wave trains are delayed relative to each other by a delay line formed by a built-in birefringence PM fibre segment, and conditions are ensured for interference of the wave trains. From the interference pattern observed on the display of a spectrum analyser with a wavelength sweep, we have determined fringe visibility as a function of wavelength, $V(\lambda)$. The results demonstrate that, at high resolutions (small $\delta\lambda$), the visibility $V(\lambda)$ is constant within the spectrum of the source and depends only on $\delta\lambda$, i.e. on the relationship between the coherence time of wave trains and the delay time. With decreasing resolution (increasing $\delta\lambda$), starting at $\delta\lambda = \delta\lambda_{hom} = 0.5$ nm the visibility $V(\lambda)$ drops sharply and becomes dependent on the wavelength in the spectrum of the light source. This strongly suggests that the homogeneous spectral width of the source lies in the range $0.2 < \delta\lambda_{hom} < 0.5$ nm and that the coherence time of wave trains corresponding to this bandwidth lies in the range $1.6 \times 10^{-11} < \tau < 4.0 \times 10^{-11}$ s. The present results give grounds to believe that the excess noise of a broadband light source is determined by not only the width of its inhomogeneous emission spectrum but also its structure. However, further research is needed to validate this conclusion.

Acknowledgements. This work was supported by the RF Ministry of Science and Higher Education (state task for the Kotelnikov Institute of Radio Engineering and Electronics, Russian Academy of Sciences).

References

1. Gubin V.P., Isaev V.A., Morshnev S.K., et al. *Quantum Electron*., **36** (3), 287 (2006) [*Kvantovaya Elektron*., **36** (3), 287 (2006)].
2. Guattari F., Chouvin S., Molucon C., Lefevre H., in *Proc. 2014 DGON Inertial Sensors and Systems* (ISS, IEEE, 2014) P10, pp 1–14.
3. Cummins H.Z., Swinney H.L. *Prog. Opt*., **8**, 133 (1970).
4. Hodara H. *Proc. IEEE*, **53** (7), 696 (1965).
5. Personov R.I., Al'shits E.I., Bykovskaya L.A. *JETP Lett*., **15**, 431 (1972) [*Pis'ma Zh. Eksp. Teor. Fiz*., **15**, 609 (1972)].
6. Kharlamov M., Personov R.I., Bykovskaya L.A. *Opt.Commun*., **12**, 191 (1974).
7. Gorokhovskii A.A., Kaarli R.K., Rebane L.A. *JETP Lett*., **20**, 216 (1974) [*Pis'ma Zh. Eksp. Teor. Fiz*., **20**, 474 (1974)].
8. Moerner W.E., Kador L. *Phys. Rev. Lett*., **62**, 2535 (1989).
9. Orrit M., Bernard J. *Phys. Rev. Lett*., **65**, 2716 (1990).
10. Wysocki P.F., Digonnet M.J.F., Kim B.Y., Shau H.J. *J. Lightwave Technol*., **12** (3), 550 (1994).
11. Andreev A.A. *Fiz. Tverd. Tela*, **46** (6), 972 (2003).
12. Wang L.A., Chen C.D. *IEEE Photonics Technol. Lett*., **9** (4), 446 (1997).
13. Sivukhin D.V. *Obshchii kurs fiziki. Optika* (A Course of General Physics: Optics) (Moscow: Nauka, 1980).
14. Mandel L., Wolf E. *Optical Coherence and Quantum Optics* (Cambridge: Cambridge Univ. Press, 1995; Moscow: Fizmatlit, 2000).
15. Mandel L., Wolf E. *Proc. Phys. Soc*., **80**, 894 (1962).
16. Morshnev S.K., Gubin V.P., Starostin N.I., Przhiyalkovskiy Ya.V., Sazonov A.I. *Foton-Ekspress*, **6** (158), 38 (2019).
17. Kikuchi K., Okoshi T. *Opt. Lett*., **8**, 122 (1983).
18. Belovolov M.I., Dianov E.M., Kryukov A.P., Pencheva V.Kh. *Tr. Inst. Obshch. Fiz., Akad, Nauk SSSR*, **15**, 164 (1988).